Motion Compensation and Efficient Array Design for TDMA FMCW MIMO Radar Systems

Christian M. Schmid, Reinhard Feger, Clemens Pfeffer, Andreas Stelzer

Christian Doppler Laboratory for Integrated Radar Sensors
Institute for Communications Engineering and RF-Systems
Johannes Kepler University Linz
Altenberger Straße 69, 4040 Linz, Austria
c.schmid@nthfs.jku.at

***Abstract*—In this paper we present methods for the design of planar frequency-modulated continuous-wave (FMCW) multiple-input multiple-output (MIMO) arrays with an emphasis on the problem of moving targets in time-division multiple-access (TDMA) systems. We discuss the influence of target motion and boundaries of operation and present a method to compensate for its effects, which requires special attention in the array design and in signal processing. Array design techniques, examples including an implementation, and measurement results are also covered in this article.**

***Index Terms*—FMCW, millimeter-wave, radar, TDMA, MIMO, array, design.**

I. Introduction

Frequency-modulated continuous-wave (FMCW) systems at millimeter wave frequencies have gained a huge interest in recent years. With monolithic microwave integrated circuit (MMIC) developed for mass markets like the automotive industry [1] they are also becoming available for other smaller volume applications [2]. The high frequencies and the high integration levels allow for these systems to become smaller and smaller which enables and drives the use of multiple antennas for transmitting and receiving to achieve an improved angular resolution capability.

In this paper we present design concepts and signal processing methods for multiple-input multiple-output (MIMO) time-division multiple-access (TDMA) arrays with a special focus on target motion, as well as an implementation. In section II we discuss a signal model for FMCW MIMO radar systems and the associated virtual antenna concept. The TDMA method for such systems including the effects of target displacement during the measurements are presented in section III. We also present array design requirements and a signal processing method to reduce these effects. Boundaries of operation of this simple method are also provided. In section IV we present design methods, for which an implementation with measurement results is presented in section V.

II. Signal Model and Virtual Array

Because of the ease of manufacturing arrays on printed circuit boards (PCBs) we will focus on planar arrays. A MIMO array is an array of antennas where multiple antennas are used for transmitting a signal (TX) and where also multiple antennas are used for receiving (RX). When TX and RX are collocated we talk about transceivers (TRXs). Fig. 1 shows such an array in the x-y plane, with a target at $(r_\mathrm{t}, \theta_\mathrm{t}, \varphi_\mathrm{t})$ and two TX, and two RX antennas at positions $\mathbf{x}=[x, y]^\mathrm{T}$.

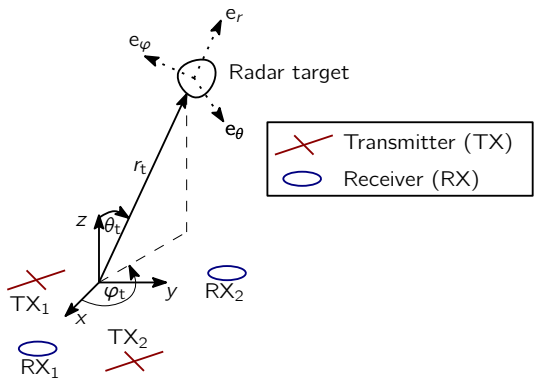

Fig. 1. A two-dimensional MIMO array consisting of two transmitters (TX) and two receivers (RX).

Assuming the radar target is in the array far-field, an FMCW system [3] signal model of the m_RXth RX channel due to a signal transmitted by the m_TXth transmit antenna is given by

$$s_\mathrm{IF}(n, m_\mathrm{TX}, m_\mathrm{RX}) = A \underbrace{\mathrm{e}^{\mathrm{j}2\pi \frac{f_0}{\mathrm{c}_0}[\mathbf{x}_\mathrm{TX}(m_\mathrm{TX})+\mathbf{x}_\mathrm{RX}(m_\mathrm{RX})]\cdot\mathbf{u}_\mathrm{t}}}_{a} \underbrace{\mathrm{e}^{\mathrm{j}4\pi \frac{B}{N\,\mathrm{c}_0}\, r_\mathrm{t}\, n}}_{b} \underbrace{\mathrm{e}^{\mathrm{j}\left(2\pi \frac{f_0}{\mathrm{c}_0}\, 2\, r_\mathrm{t}+\Phi_\mathrm{t}\right)}}_{c}. \quad (1)$$

with

$$\mathbf{u}_\mathrm{t} = \left[\sin\theta_\mathrm{t}\cos\varphi_\mathrm{t},\, \sin\theta_\mathrm{t}\sin\varphi_\mathrm{t}\right]^\mathrm{T}, \quad (2)$$

where B is the FMCW signal bandwidth, c_0 is the speed of light, $n{=}0\ldots N{-}1$ is the sample index and with Φ_t being an unknown target reflection phase.

If it is possible to separately measure all TX and RX combinations, we obtain $M_\mathrm{TX}{\times}M_\mathrm{RX}$ signals. In this case a MIMO setup can be equivalently substituted by a single transmit antenna at $\mathbf{x}{=}[0,0]^\mathrm{T}$ and by $M_\mathrm{TX}{\times}M_\mathrm{RX}$ receive antennas. This equivalent multiple-input single-output antenna array setup is called the virtual array with the virtual antenna

positions

$$\mathbf{x}_{\mathrm{V}}(m_{\mathrm{TX}}, m_{\mathrm{RX}}) = \mathbf{x}_{\mathrm{TX}}(m_{\mathrm{TX}}) + \mathbf{x}_{\mathrm{RX}}(m_{\mathrm{RX}}). \quad (3)$$

The virtual antenna concept is an important tool for designing a MIMO array as it provides the link between MIMO arrays and classical array synthesis techniques. The MIMO array has the same properties as its virtual counterpart RX only array, assuming that the target position does not change during the measurements. Fig. 2 shows a MIMO array and its associated virtual array according to (3). The advantages of the MIMO concept are obvious as the virtual array has a higher number of elements than the original array and as the aperture of the virtual array is also larger than that of the original array.

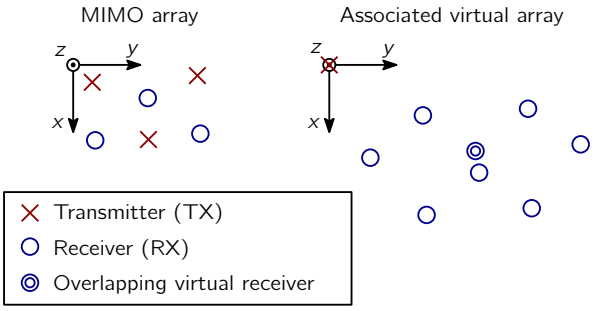

Fig. 2. A MIMO array and its associated virtual array according to (3).

While a MIMO array results in an associated virtual array of $M_{\mathrm{V}}{=}M_{\mathrm{TX}}{\times}M_{\mathrm{RX}}$ elements, the virtual antenna positions might not be unique. For example a TRX MIMO system may only result in a virtual array with up to $M_{\mathrm{Vu}}{\leq}M_{\mathrm{TRX}} \times (M_{\mathrm{TRX}}{+}1)/2$ unique positions [4]. It is certainly desirable to design a MIMO array in a way to obtain the maximum number of unique virtual antenna positions. On the other hand virtual antennas that do not have unique positions (we shall call them overlapping virtual antennas) can be used to compensate moving target effects in TDMA FMCW MIMO radar systems.

III. TDMA and Displacement Compensation for MIMO Arrays

The virtual array model of section II requires that all TX and RX combinations can be measured separately. There are multiple ways to achieve such a seperation such as

- TDMA,
- Frequency-division multiple-access and
- Code-division multiple-access.

For TDMA the TXs are enabled sequentially. One complete MIMO measurement is split up into M_{TX} measurement cycles with only one TX active at a time. It is the simplest form, with the lowest requirements regarding the hardware and works well, when the targets do not move between the measurement cycles.

A. Phase Shift due to Moving Targets

The conventional delay-and-sum beamforming requires a signal in the form of (1). If a target is moving, its position changes during the sequential TX activations and the resulting radar image may become blurry [2] or completely useless, as shown in Fig. 3.

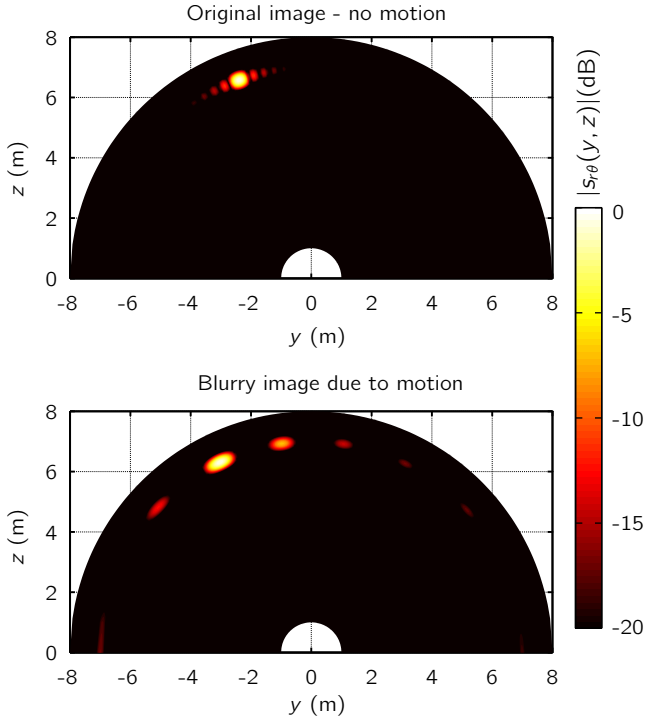

Fig. 3. Effects of a moving target: The radar image becomes blurry or even completely useless.

We will now consider target displacements with respect to the target coordinate system in Fig. 1. Similar to the antenna far-field condition, that is often defined by a maximum phase error of $\pi/8$ [5], we will discuss this condition in the context of target motion.

1) Displacement in $\mathbf{e}_\varphi$ or $\mathbf{e}_\theta$ direction: Analyzing (1) reveals that a change in φ_{t} and θ_{t} will only influence the spatial frequency term a. If

$$2\,\pi f_0/\mathrm{c}_0\,[D_x\;D_y]\,\Delta\mathbf{u}_{\mathrm{t}} \leq \pi/8 \quad (4)$$

the effects due to a target displacement in $\mathbf{e}_\varphi$ or $\mathbf{e}_\theta$ can be neglected, with D_i denoting the respective array aperture dimensions and with $\Delta\mathbf{u}_{\mathrm{t}}$ denoting the change of $\mathbf{u}_{\mathrm{t}}$ during the measurement cycle. For a 77-GHz uniform $\lambda/2$ linear 8 elements array (where λ is the free-space wavelength) this leads to $\Delta u \leq 0.016$ and via geometrical relations for a target at $r_{\mathrm{t}}{=}10$ m with a measurement cycle of $T{=}4$ ms to a target velocity of $v_{\max}{=}40$ m/s.

2) Displacement in $\mathbf{e}_r$ direction: A change of r_{t} effects b as well as c in (1). Considering the term b we find

$$4\pi B/\mathrm{c}_0\,\Delta r_{\mathrm{t}} \leq \pi/8, \quad (5)$$

which, for a bandwidth of $B{=}500$ MHz and with the setup from 1), results in a maximum velocity of $v_{\max}{=}4.7$ m/s.

The most sensitive part in terms of target motion is c for which we find

$$4\pi f_0/\mathrm{c}_0\,\Delta r_{\mathrm{t}} \leq \pi/8. \quad (6)$$

For the 77-GHz system with T=4 ms this means that $v_{\max}$=0.03 m/s. While $\pi/8$ might be a conservative boundary, we see that for typical 77-GHz TDMA FMCW MIMO systems the change of c due to radial target motion has the most crucial influence.

B. Moving Target Phase Compensation

We will now focus on compensating the effect of changing phases during the sequential TDMA measurements. To account for them we can extend (1) to

$$\tilde{s}_{\mathrm{IF}}(n, m_{\mathrm{TX}}, m_{\mathrm{RX}}) = s_{\mathrm{IF}}(n, m_{\mathrm{TX}}, m_{\mathrm{RX}})\, c_{m_{\mathrm{TX}}}, \qquad (7)$$

with the unknown complex phase coefficients $c_{m_{\mathrm{TX}}}$. When we have two measurements from different different TX $m_{\mathrm{TX}i}$, $m_{\mathrm{TX}j}$ and for two different RX $m_{\mathrm{TX}k}$, $m_{\mathrm{TX}l}$ where the ideal signal model is identical

$$s_{\mathrm{IF}}(n, m_{\mathrm{TX}i}, m_{\mathrm{RX}k}) = s_{\mathrm{IF}}(n, m_{\mathrm{TX}j}, m_{\mathrm{RX}l}), \qquad (8)$$

and assuming that the amplitude does not change, we can find the relative phase shift between these two measurements

$$\frac{\tilde{s}_{\mathrm{IF}}(n, m_{\mathrm{TX}i}, m_{\mathrm{RX}k})}{\tilde{s}_{\mathrm{IF}}(n, m_{\mathrm{TX}j}, m_{\mathrm{RX}l})} = \frac{c_{m_{\mathrm{TX}i}}}{c_{m_{\mathrm{TX}j}}}. \qquad (9)$$

By correcting one of the two measurement cycles by this factor it is possible to establish phase coherence between the two cycles even when the target position has changed. In terms of the virtual antenna concept the TX and RX combinations where the signal model is identical can be interpreted as overlapping virtual antennas. Thus we need to pay attention in the array design to be able to perform this kind of phase compensation.

The problem can be interpreted in the context of graph theory by a graph with M_{TX} nodes, where each node represents a measurement cycle and where each edge represents a pair of overlapping virtual antennas. In order to establish phase coherence between all measurement cycles we require a graph that admits a spanning tree. We therefore need a minimum of $M_{\mathrm{TX}} - 1$ properly designed pairs of overlapping antennas in order to be able to find a spanning tree. An exemplary array and its graph representation is given in Fig. 4.

It becomes obvious that the problem does not have a unique solution as there exist a multitude of spanning trees for a MIMO array with $M_{\mathrm{TX}} \geq 3$ and also a multitude of potential overlapping virtual RX elements depending on the array design. A virtual array that allows for the presented phase compensation has a number of unique virtual antenna positions of

$$M_{\mathrm{Vu}} \leq M_{\mathrm{Vu,max}} = M_{\mathrm{TX}} \times M_{\mathrm{RX}} - (M_{\mathrm{TX}} - 1), \qquad (10)$$

with $M_{\mathrm{Vu,max}}$ being the maximum number of unique antenna positions, for which compensation is possible.

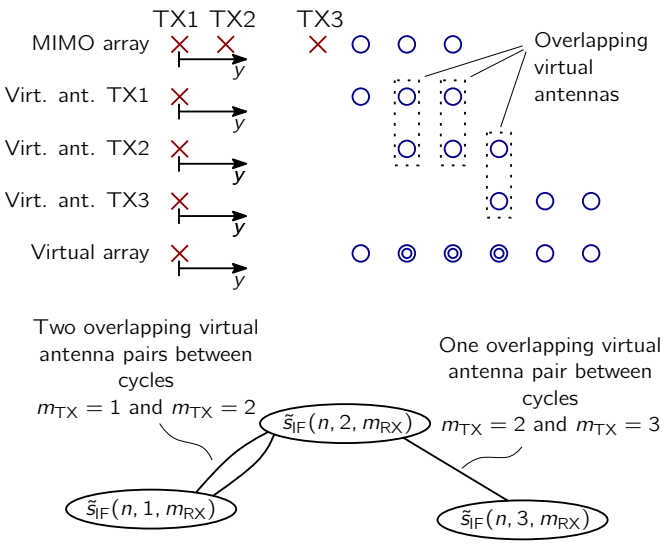

Fig. 4. A 3-TX 3-RX MIMO array with three overlapping virtual antennas and its graph representation showing the measurement cycles (nodes) and the overlapping virtual antenna pairs (edges).

C. Frequency Shift due to Moving Targets

So far we have only considered the phase shift of the different components in (1). However also the frequency in term b changes due to the target displacement during the TX cycles. Fig. 5 shows the magnitude of the temporal discrete Fourier transform $S_{\mathrm{IF}}(x)$=DFT $\{w(n)\, s_{\mathrm{IF}}(n)\}$ of an RX channel for different TX activation cycles while a target is moving, where $w(n)$ denotes the temporal window function.

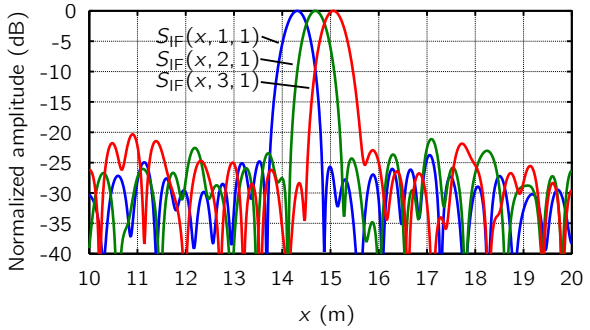

Fig. 5. The frequency shifts for a moving target during the sequential TX activation.

The faster a target moves the more the peaks are going to be separated. The width of a peak is defined by the radar's resolution capability [6] and thus

$$\alpha\, 2c_0/B, \qquad (11)$$

where α accounts for the window function $w(n)$ [7]. It is reasonable to demand that all peaks have to overlap significantly during one complete radar measurement, so that

$$\Delta r_{\mathrm{t}} < \alpha\, c_0/B. \qquad (12)$$

Assuming a constant velocity during the measurement, a rectangular window and the exemplary system with T=4 ms

and B=500 MHz this leads to a relaxed boundary of $v_{\max} < 150$ m/s.

IV. MIMO Array Design

In this section we present design techniques that provide the required overlapping virtual array elements for the presented motion phase compensation concept.

A. TRX Arrays

In a TRX array where each antenna is used for transmitting and for receiving, so that

$$\mathbf{x}_{\mathrm{TX}}(m) = \mathbf{x}_{\mathrm{RX}}(m) = \mathbf{x}_{\mathrm{TRX}}(m), \tag{13}$$

there are enough overlapping virtual antennas automatically, as

$$s_{\mathrm{IF}}(n, m_i, m_j) = s_{\mathrm{IF}}(n, m_j, m_i). \tag{14}$$

However the virtual antenna setup is not optimal in a sense that there are at least $M_{\mathrm{TRX}}(M_{\mathrm{TRX}}-1)/2$ overlapping antennas which is more than required and thus $M_{\mathrm{Vu}} < M_{\mathrm{Vu,max}}$.

B. Linear Antenna Arrays

We assume that the antenna array is located on the y-axis with antenna positions $\mathbf{x}$=$[0, y]^{\mathrm{T}}$. If we assume a given RX configuration and design the TX array in a way so that

$$y_{\mathrm{TX}}(m+1) - y_{\mathrm{TX}}(m) = y_{\mathrm{RX}}(M_{\mathrm{RX}}) - y_{\mathrm{RX}}(1), \tag{15}$$

we will get the required overlapping virtual antennas, as for consecutive TX measurements the virtual antenna positions from the last RX and from the first RX respectively overlap

$$y_{\mathrm{TX}}(m+1) + y_{\mathrm{RX}}(1) = y_{\mathrm{TX}}(m) + y_{\mathrm{RX}}(M_{\mathrm{RX}}). \tag{16}$$

Thus we have

$$s_{\mathrm{IF}}(n, m, M_{\mathrm{RX}}) = s_{\mathrm{IF}}(n, m+1, 1). \tag{17}$$

A minimum number of $M_{\mathrm{TX}} - 1$ virtual antennas is spent to realize the phase compensation, all other virtual antennas are used to span the aperture, thus M_{Vu}=$M_{\mathrm{Vu,max}}$. While this approach restricts the TX array to a uniform array, it can be used to design an efficient fully filled uniform linear array as shown in Fig. 6

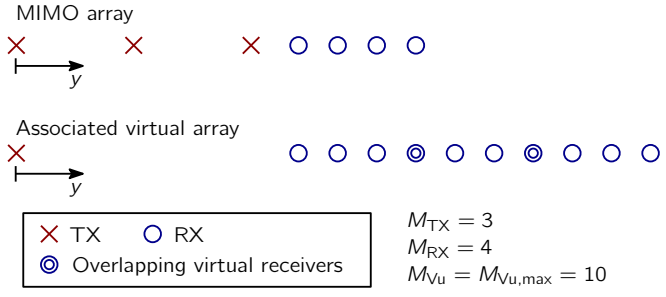

Fig. 6. A linear MIMO array, that leads to a uniform virtual array, with the minimum number of overlapping virtual antennas required for motion compensation.

C. 2d Arrays

Another approach that works for arbitrary 3d arrays and yields the required overlapping virtual antennas is to enforce one virtual antenna to be at the same position for all measurement cycles, so that for any measurement cycles $m_{\mathrm{TX}i}$ and $m_{\mathrm{TX}j}$ there exists exactly a virtual antenna position

$$\begin{aligned}\mathbf{x}_{\mathrm{TX}}(m_{\mathrm{TX}i}) + \mathbf{x}_{\mathrm{RX}}(m_{\mathrm{RX}k}) = \\ = \mathbf{x}_{\mathrm{TX}}(m_{\mathrm{TX}j}) + \mathbf{x}_{\mathrm{RX}}(m_{\mathrm{RX}l}) = \mathbf{x}_{\mathrm{Vconst}}.\end{aligned} \tag{18}$$

The equation above is automatically fulfilled if for every TX element there exists an RX element with position

$$\mathbf{x}_{\mathrm{RX}} = \mathbf{x}_{\mathrm{Vconst}} - \mathbf{x}_{\mathrm{TX}}, \tag{19}$$

in other words, when there is a subset in the RX array that is a geometrically mirrored version of the TX array. This does however not ensure that there are not more overlapping elements than required.

As it is shown in Fig. 7 the presented approach can be realized using a multiplexer to minimize the number of required RX RF and/or baseband channels.

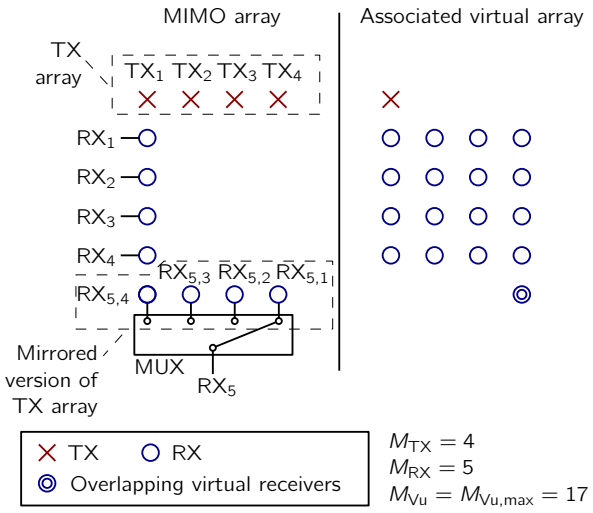

Fig. 7. A 2d MIMO array with 4 TX and 5 RX channels that leads to a virtual array with 17 unique virtual antenna positions.

In Fig. 7 the multiplexer is set to $\mathrm{RX}_{5,i}$ when TX_i is activated, so that

$$\mathbf{x}_{\mathrm{TX}}(m_{\mathrm{TX}}) + \mathbf{x}_{\mathrm{RX}}(5) = \mathbf{x}_{\mathrm{Vconst}}. \tag{20}$$

As the TX array in Fig. 7 is uniform and thus is identical when mirrored, using TRX instead of TX elements is also an option.

Again the virtual array has a maximum obtainable number of unique, virtual antenna positions of M_{Vu}=$M_{\mathrm{Vu,max}}$.

V. Implementation and Measurement Results

TRX TDMA MIMO systems can be found in [4], [8], they all offer the phase calibration capability as described in IV-A. We will now present the implementation of an array designed according to IV-B which is shown in Fig. 8.

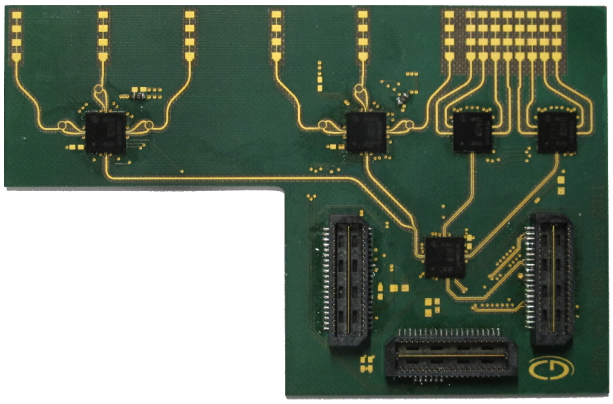

Fig. 8. An implementation of a 77-GHz TDMA FMCW MIMO radar system designed according to section IV-B.

This 77-GHz FMCW radar system consists of M_{TX}=6 TX channels and M_{RX}=8 RX channels with SiGe MMICs by Infineon. The RX antennas have a spacing of 1.9 mm ($\approx\lambda/2$) and the TX antennas are separated by 7×1.9 mm=13.3 mm. The resulting virtual array is a linear, uniform, $\lambda/2$ array, similar to Fig. 6, but with 43 unique antenna positions and 5 overlapping antenna pairs for phase compensation.

To verify the proposed array design and the algorithm we mounted a corner cube reflector as target onto a computer-controlled, linear rail running perpendicular to the MIMO array and performed measurements for different target velocities v_{target}. The FMCW radar parameters are summarized in Table I.

TABLE I
SUMMARY OF THE PARAMETER SETTINGS FOR THE FMCW RADAR MEASUREMENTS.

Start frequency	f_0	74 GHz
Bandwidth	B	2 GHz
Ramp duration	T_{r}	1 ms
Sampling rate	f_{s}	1.25 MS/s

As in the implemented system one TX measurement cycle consists of an up- and a downchirp, the complete measurement takes T=6×2 ms=12 ms. Fig. 9 show measurement results for a target at v_{target}=3 m/s without and with the compensation technique presented in III-B, which is required as (6) is violated. Using a Hann window a change in frequency can be neglected, in accordance with (12), as long as the target velocity is well below $v_{\mathrm{max}}\approx$25 m/s. One can clearly see how the blurry image of a single target can be reconstructed.

VI. Conclusion

In this paper we presented the problem of moving target scenarios in TDMA FMCW MIMO radar systems. We analyzed the effects of moving targets and provided a method to compensate for unknown phase shifts. The method requires special attention in the array design which we covered and explained by means of the virtual antenna concept, which provides a link between classical array theory and MIMO arrays.

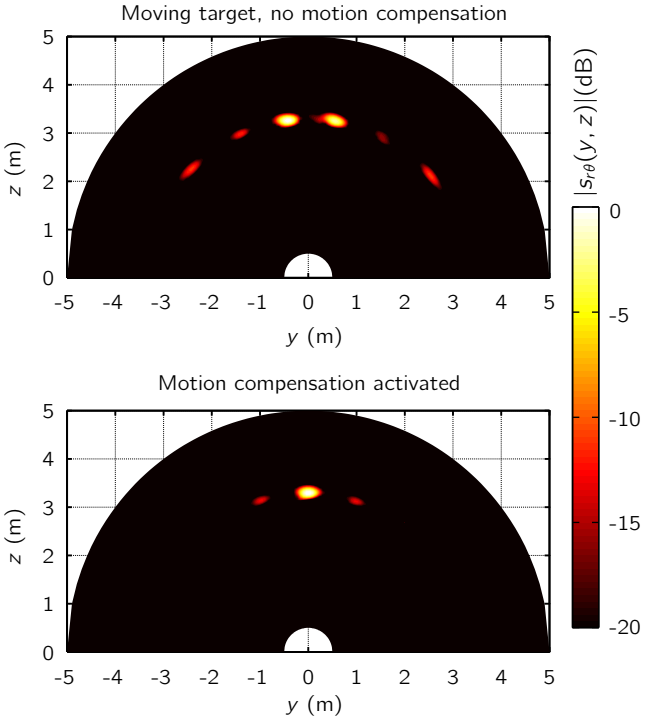

Fig. 9. Measurement results for a target moving at a velocity of v_{target}=4 m/s, without and with the motion compensation technique presented.

We presented three design approaches and an implementation including measurement results.

Acknowledgement

The authors wish to acknowledge the Christian Doppler Research Association, DICE GmbH & Co KG as part of the Infineon group for funding this work carried out at the Christian Doppler Laboratory for Integrated Radar Sensors and also for providing the 77-GHz SiGe MMICs.

References

[1] A. Stelzer, R. Feger, and M. Jahn, "Highly-integrated multi-channel radar sensors in SiGe technology for automotive frequencies and beyond," in *ICECom, 2010 Conference Proceedings*, sept. 2010, pp. 1 –11.

[2] S. S. Ahmed, A. Schiessl, and L.-P. Schmidt, "A novel fully electronic active real-time imager based on a planar multistatic sparse array," *Microwave Theory and Techniques, IEEE Transactions on*, vol. PP, no. 99, p. 1, 2011.

[3] A. Stove, "Linear FMCW radar techniques," *IEE Proceedings F Radar and Signal Processing,*, vol. 139, no. 5, pp. 343 –350, Oct 1992.

[4] R. Feger, C. Wagner, S. Schuster, S. Scheiblhofer, H. Jager, and A. Stelzer, "A 77-GHz FMCW MIMO radar based on an SiGe single-chip transceiver," *IEEE Transactions on Microwave Theory and Techniques,*, vol. 57, no. 5, pp. 1020 –1035, May 2009.

[5] C. A. Balanis, *Antenna Theory: Analysis and Design*, 3rd ed. Hoboken, NJ: John Wiley & Sons, 2005.

[6] A. W. Rihaczek, *Principles of High-Resolution Radar*. Los Altos, California, US: Peninsula Publishing, 1985.

[7] F. Harris, "On the use of windows for harmonic analysis with the discrete fourier transform," *Proceedings of the IEEE*, vol. 66, no. 1, pp. 51 – 83, jan. 1978.

[8] C. Schmid, R. Feger, C. Wagner, and A. Stelzer, "Design of a linear non-uniform antenna array for a 77-GHz MIMO FMCW radar," in *MTT-S International Microwave Workshop on Wireless Sensing, Local Positioning, and RFID, IEEE*, Sep. 2009.